Strange attractors and chaotic motions of dynamical systems

Edward Ott

Department of Physics and Astronomy, University of Maryland, College Park, Maryland 20742
and Department of Electrical Engineering, University of Maryland, College Park, Maryland 20742

A review is presented of recent work related to strange attractors and chaotic motions of dynamical systems. First, simple systems capable of displaying chaotic behavior are discussed. In order of increasing dimensionality of the system, they are one-dimensional noninvertible maps, two-dimensional invertible maps, and autonomous systems of three coupled ordinary differential equations. The concept of fractional dimension of the strange attractor is stressed. Several physical examples well be reviewed, along with the possible relevance to turbulence in systems, such as fluids or plasmas, that are described by partial differential equations.

CONTENTS

I. INTRODUCTION

In this report, a review will be presented of recent developments related to strange attractors and chaotic motions of dynamical systems. Emphasis will be placed on those aspects that may prove useful for physical scientists.

At this point it might be appropriate to discuss some of the terms used in the title. A *dynamical system* may be thought of as any set of equations giving the time evolution of the state of a system from a knowledge of its previous history. Examples are Maxwell's equations, the Navier-Stokes equations, and Newton's equations of motion for a particle with suitably specified forces. The adjective *chaotic* is used here to describe a type of time evolution resulting from a dynamical system. In particular, it describes motions which are commonly thought of as "turbulent," i.e., motions whose time evolution appears, on detailed examination, to be very complex. For such motions, one often has the feeling that a statistical description may be of more use than actual knowledge of the true evolution. (A more precise definition of the term *chaotic* appears in Sec. II.) At this point I shall not attempt to define a *strange attractor.* Rather, we only note that its presence can lead to chaotic motion. Thus, the topic under discussion in this review is related to the occurrence of turbulent-type motions in physical systems. More specifically, we shall be concerned with nonconservative systems. [Chaotic motion in Hamiltonian (conservative) systems is not within the scope of the present review.]

It is becoming increasingly clear that the topic of strange attractors is one that will find abundant applications in a wide variety of physical situations. The list of such applications is already large, including problems in the onset of turbulence in fluids (Lorenz, 1963; McLaughlin and Martin, 1975; Ruelle and Takens, 1971), chemically reacting systems (Tomita and Kai, 1979), buckling beams (Holmes, 1980), nonlinear wave interactions in plasmas (Adam, Bussac, and Laval, 1980; Wersinger, Finn, and Ott, 1980a, 1980b, 1980c; Vyshkind, 1978; Vyshkind and Rabinovich, 1976; Russell and Ott, 1980; Wang, 1980; Masui and Wang, 1980), solid-state physics (Huberman and Crutchfield, 1979), lasers (Haken, 1975), self-generation of the earth's magnetic field (Robbins, 1977), magnetohydrodynamic flow (Maschke and Saramito, 1980; Treve and Manley, 1980), etc. (The above is only a partial listing and many other relevant references exist.)

As can be surmised from the dates of the references just mentioned, virtually all the activity in this field (at least when restricted to problems in the physical sciences) has occurred since 1975. The notable exceptions to this statement are the papers of Lorenz (1963) and of Ruelle and Takens (1971). These two papers, independently and from quite different points of view, originally suggested the relevance of strange attractors to the onset of turbulence in fluid flows. Lorenz was interested in explaining the presence of chaotic behavior in numerical solutions of a model system of three coupled, first-order, nonlinear, ordinary differential equations which modeled the nonlinear evolution of the Benard instability, i.e., the instability which results when a fluid layer subjected to gravity is heated sufficiently strongly from below. By a combination of careful analysis of the computer generated solutions and analytical reasoning, Lorenz was able to deduce that the solution of his equations was eventually trapped in a region of the phase space of the system which had a very intricate (strange) geometric structure. The now-recognized general implications of Lorenz's paper were not widely appreciated until many years after its publication. In 1971, Ruelle and Takens, making use of

then recent developments in mathematics, offered a possible mechanism by which turbulent solutions to the Navier-Stokes equations could appear as a parameter is varied (e.g., as the Reynolds number is increased). In particular, they showed on the basis of quite general arguments that a strange attractor could appear. It is to be anticipated that the application of the type of considerations initiated by these two papers will lead to new insights in a variety of fields of physics. The purpose of the present paper is to facilitate this process by providing an elementary introduction designed for researchers and students in the physical sciences.

Some previous related reviews from various points of view are those of Treve (1978), Swinney and Gollub (1978), Rabinovich (1978), Ruelle (1977), Sinai (1977), Holmes (1977), Helleman (1980), Shaw (1981), and Yorke and Yorke (1981).

We shall proceed by discussing dynamical systems of progressively higher dimension (all of which can display chaotic behavior) [Ruelle (1977)]:

(1) One-dimensional noninvertible maps,

(2) Two-dimensional invertible maps,

(3) First-order systems of autonomous ordinary differential equations,

$$\frac{dx_i(t)}{dt} = f_i[x_1(t), x_2(t), \ldots, x_n(t)] \quad i = 1, 2, \ldots, n, \text{ with } n > 3.$$

(4) Partial differential equations.

One-dimensional maps will be discussed in the next section (Sec. II). These are relations of the form $x_{n+1} = F(x_n)$; thus, for some initial x_0, a sequence, $x_0, x_1, x_2, \ldots$, is generated. Surprisingly, very simple one-dimensional maps will turn out to yield rather good qualitative models for behavior in two-dimensional maps (Sec. III), ordinary differential equations (Sec. IV), and partial differential equations (Sec. V).

II. ONE-DIMENSIONAL NONINVERTIBLE MAPS

To begin, we consider one-dimensional maps

$$x_{n+1} = F(x_n), \tag{2.1}$$

where $F(x)$ is a scalar function. [Some relevant references on one-dimensional maps are Li and Yorke (1975); May (1976); Guckenheimer *et al.* (1977); Feigenbaum (1978); and Guckenheimer (1979). In addition, a monograph by Coullet and Eckmann (1980) has been published on the subject.] We only consider the case in which the sequence $x_0, x_1, x_2, \ldots$, generated by F is bounded, $P < x_n < Q$, for all n. We will often say that such a sequence is "chaotic" or "turbulent," by which we mean that it has the following properties: (1) sensitive dependence on initial conditions (if two initial points x_0^a and x_0^b are chosen very close to each other, the distance between their successive images under F initially diverges exponentially); (2) the average correlation function for a given sequence satisfies $C(m) \to 0$ as $m \to \infty$, where

$$C(m) = \lim_{N\to\infty} \frac{1}{N} \sum_{n=1}^{N} (x_n - \langle x \rangle)(x_{n+m} - \langle x \rangle),$$

$$\langle x \rangle = \lim_{N\to\infty} \frac{1}{N} \sum_{n=1}^{N} x_n;$$

(3) The sequence is nonperiodic.

We now introduce the following two one-dimensional maps, each of which typifies a broad class,

$$F_1(x) \equiv a(1 - 2|x - \tfrac{1}{2}|), \quad 0 < a \leq 1 \tag{2.2}$$

$$F_2(x) = 4bx(1 - x), \quad 0 < b \leq 1 \tag{2.3}$$

where a and b are constants. The map F_1 has a sharp peak, while the map F_2 has a rounded smooth maximum. For $0 < (a, b) < 1$, both F_1 and F_2 map the interval 0 to 1 into itself, and we shall only consider this range of x (i.e., initial conditions are always assumed to satisfy $1 > x_0 > 0$). Both F_1 and F_2 are noninvertible, since, given x_{n+1}, one cannot solve $x_{n+1} = F(x_n)$ for x_n. (From Fig. 1 it is seen that for each value of x_{n+1} there are *two* possible values of x_n.) Thus one may say that it is possible to go forward in time but not backward in time. This represents a basic difference with ordinary differential equations, $\dot{\mathbf{x}} = \mathbf{f}(\mathbf{x})$, which may, in principal, be integrated either forward or backward in time.

First consider F_1. There are essentially two cases of interest, $0 < a < \frac{1}{2}$ and $\frac{1}{2} < a \leq 1$, both illustrated in Fig. 1(a). In Fig. 1, the dashed line represents $x_n = x_{n+1}$. For $0 < a < \frac{1}{2}$, Fig. 1(a) shows that $x_{n+1} < x_n$, since, over

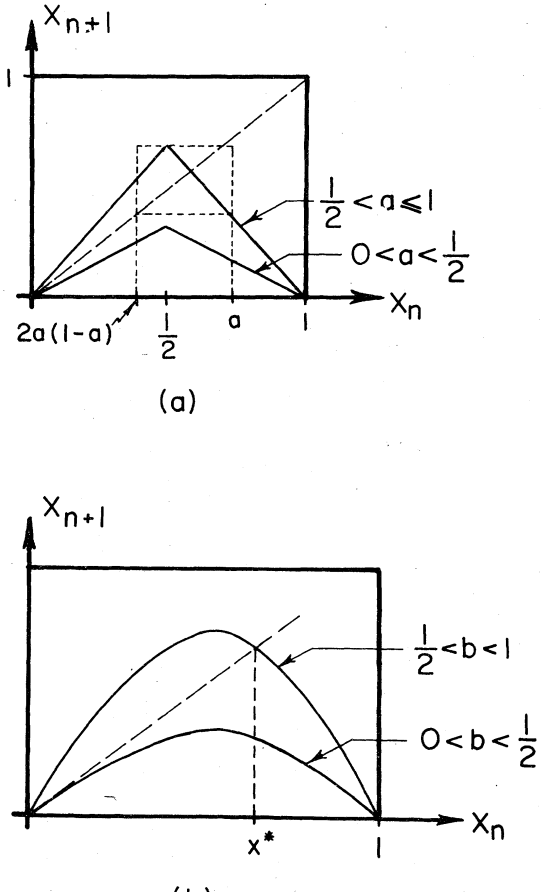

FIG. 1. (a) Map F_1 [Eq. (2.2)], and (b) the map F_2 [Eq. (2.3)].

the entire range, $F_1(x_n)$ lies below the line $x_n = x_{n+1}$. In this case it is clear that x_n converges to zero as n increases. Now, consider $\frac{1}{2} < a \leq 1$. For any initial x_0 between 0 and 1, the sequence eventually becomes trapped in the interval $2a(1-a) < x < a$ through which it will typically wander chaotically. To illustrate this, consider the particularly simple case $a = 1$ for which the chaotic interval becomes $0 < x < 1$. In this case, we may consider the map to represent two steps: (1) a uniform stretching of the interval 0 to 1 to twice its original length, and (2) a folding in half of the stretched interval so that it now has its original length. These steps are illustrated in Fig. 2. The stretching property leads to exponential separation of nearby points and hence, sensitive dependence on initial conditions. The folding property keeps the generated sequence bounded, but also causes the map to be noninvertible, since it causes two different x_n points to be mapped into one x_{n+1} point.

Conversely, for a general one-dimensional map, in order to have the distance between nearby points separate exponentially, it is necessary for the map to be, on the average, stretching. On the other hand, to have the sequence remain bounded (confined between 0 and 1 in the case of F_1), folding must take place. Thus we conclude that in order for a one-dimensional map to exhibit chaotic behavior, it must be noninvertible. Figure 3 illustrates the stretching and folding properties of F_1 for a value of a less than one ($\frac{1}{2} < a < 1$). From Fig. 3(a) we see that after one application of F_1, there are no points in $a < x < 1$. From Fig. 3(b), we see that the interval 0 to $2a(1-a)$ is stretched but that no points are folded back onto it. Thus any point in $0 < x < 2a(1-a)$ will eventually leave that interval and never return. Thus the generated sequence is eventually trapped in $2a(1-a) < x < a$. An alternative way of seeing the fact that F_1 has sensitive dependence on initial conditions is illustrated in Fig. 4 for the case $a = 1$. Figure 4(a) shows x_{n+2} versus x_n obtained from two applications of

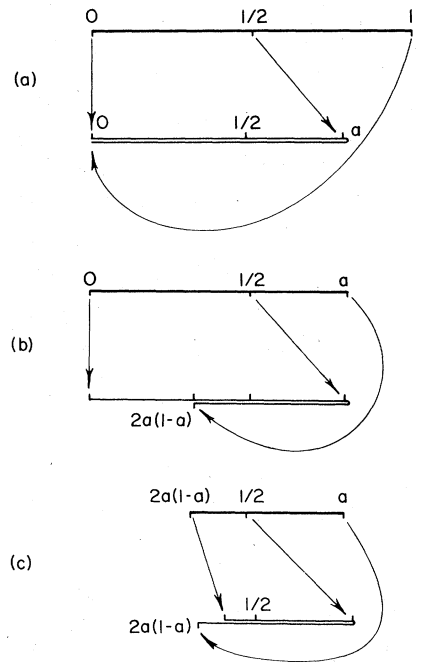

FIG. 3. Map F_1 for $a = 0.8$; (a) mapping of the interval 0 to 1, (b) 0 to a, and (c) $2a(1-a)$ to a.

F_1; that is, $x_{n+2} = F_1[F_1(x_n)]$. We will use the notation $x_{n+2} = F_1^{(2)}(x_n)$ to denote $F_1[F_1(x_n)]$. For x_{n+m} versus x_n, Fig. 4(a) generalizes to Fig. 4(b), $x_{n+m} = F_1^{(m)}(x_n)$. From Fig. 4(b), one can see that if the initial condition has an uncertainty $\pm\varepsilon$, then after $m \sim \ln_2(1/\varepsilon)$ iterations of F_1, we will have essentially no clue as to where x lies in the interval 0 to 1 (example: for $\varepsilon \cong 10^{-12}$, $m \cong 40$).

We now turn to a consideration of the map F_2 [Eq.

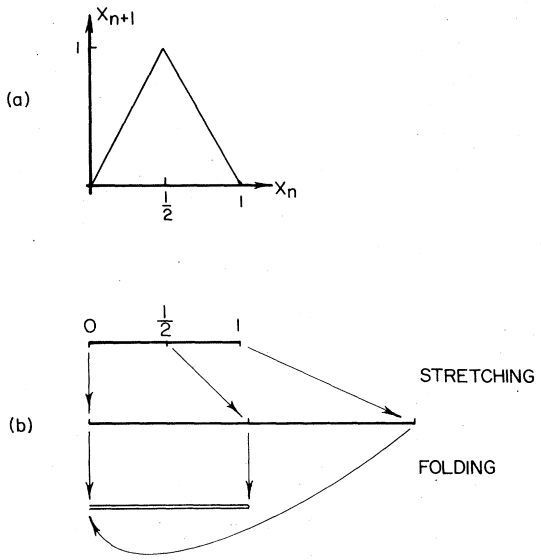

FIG. 2. (a) F_1 map at $a = 1$. (b) Illustration of the stretching and folding properties of F_1 for $a = 1$.

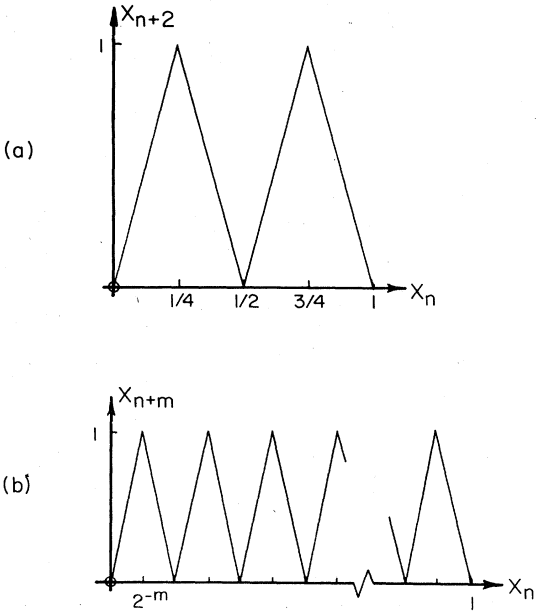

FIG. 4. (a) x_{n+1} vs x_n for F_1 with $a = 1$. (b) x_{n+m} vs x_n for F_1 with $a = 1$ (the length along the x_n axis is expanded).

(2.3) and Fig. 1(b)], which has a smooth rounded maximum at $x_n=\frac{1}{2}$ as opposed to the sharp peak in F_1 [Fig. 1(a)]. From Fig. 1(b) we note that the line $x_n=x_{n+1}$ intersects the map at $x_n=0$ for $0<b<\frac{1}{2}$ and at two points, $x_n=0$ and $x_n=x^*$, for $\frac{1}{2}<b<1$, where, from (2.3), $x^*=1-(4b)^{-1}$. These points of intersection are fixed points of the map; that is, if the initial point is chosen to be a fixed point, then successive applications of the map leave it unmoved. It is important to discover whether the fixed points are stable to small perturbations. Let $\bar{x}$ be a fixed point, $\bar{x}=F(\bar{x})$, and consider a perturbation from it, $x_n=\bar{x}+\delta_n$. From (2.1), $\bar{x}+\delta_{n+1}=F(\bar{x}+\delta_n)$. For δ_n small, we can Taylor-series expand $F(\bar{x}+\delta_n)$ as $F(\bar{x})+F'(\bar{x})\delta_n=\bar{x}+F'(\bar{x})\delta_n$, from which we obtain

$$\delta_{n+1}/\delta_n=F'(\bar{x})\,, \tag{2.4}$$

where $F'\equiv dF/dx$. Thus, if $|F'(\bar{x})|>1$, images under F of points near $\bar{x}$ successively move farther away from it, and $\bar{x}$ is unstable. For $|F'(\bar{x})|<1$, points near $\bar{x}$ converge to it, and $\bar{x}$ is stable. (For example, for F_1 given by Eq. (2.2), $|F_1'(x)|=2a$ for $x\neq\frac{1}{2}$, and thus $\bar{x}=0$ is stable for $0<a<\frac{1}{2}$, while zero and the second intersection [cf. Fig. 1(a)] are both unstable for $\frac{1}{2}<a\leq 1$.) For F_2, Eq. (2.3) shows that $F'(0)=4b$, and $F'(x^*)=2(1-2b)$. Thus, zero is stable for $b<\frac{1}{4}$. The fixed point $x=x^*$ first appears at $b=\frac{1}{4}$, and, simultaneously with its appearance, the zero fixed point loses its stability. The fixed point $x^*=1-(4b)^{-1}$ is stable in $\frac{3}{4}>b>\frac{1}{4}$, since $|F'(x^*)|<1$ in this range. Corresponding to these results, it can be shown that the sequence generated by F_2 converges to zero for $0\leq b<\frac{1}{4}$ and to x^* for $\frac{1}{4}<b<\frac{3}{4}$. $F'(x^*)=1$ at $b=\frac{1}{4}$ and decreases as b increases, becoming zero at $b=\frac{1}{2}$, minus one at $b=\frac{3}{4}$, and less than minus one (unstable) for $b>\frac{3}{4}$. The question which then arises is what happens in the range $\frac{3}{4}<b<1$ for which both 0 and x^* are unstable. To begin answering this question it is instructive to examine the map $x_{n+2}=F_2^{(2)}(x_n)$ shown in Fig. 5 for b slightly below $\frac{3}{4}$ and for b slightly above $\frac{3}{4}$. Values of x which recur every second iteration, i.e., in a series $e,f,e,f,e,f,\ldots$ are fixed points of $F^{(2)}$, $e=F^{(2)}(e)$, and $f=F^{(2)}(f)$, with $e=F(f)$ and $f=F(e)$. For the special case $e=f$, e will also be a fixed point of F itself. Now consider the stability of the sequence $e,f,e,f,\ldots$. Taking $x_n=e+\delta_n$, $x_{n+2}=e+\delta_{n+2}$, we have $e+\delta_{n+2}=F^{(2)}(e+\delta_n)=F[F(e+\delta_n)]$, which, when Taylor-series expanded, yields

$$\delta_{n+2}/\delta_n=F'(e)F'(f)=F^{(2)\prime}(e)=F^{(2)\prime}(f)\,. \tag{2.5}$$

Applying (2.5) to a fixed point of F, we have $F^{(2)\prime}(x^*)=[F'(x^*)]^2$. Thus, when x^* loses stability, the slope of $F^{(2)}$ at x^* becomes greater than one. Referring, now, to Fig. 5 for F_2, it is seen that, when this occurs, two new intersections of $F_2^{(2)}$ with $x_{n+2}=x_n$, e and f, simultaneously appear. Furthermore, when these points appear, they initially have $F_2^{(2)\prime}(e)=F_2^{(2)\prime}(f)=1$, and the slopes decrease as b is raised. Thus, the new fixed points of $F^{(2)}$ are initially stable, and it is found that, when b slightly exceeds $\frac{3}{4}$, the generated sequence converges to an alternating one, $e,f,e,f,\ldots$. As b increases further, however, $F_2^{(2)\prime}(e)=F_2^{(2)\prime}(f)$ decreases; eventually, past $b=0.862\ldots$, $F_2^{(2)\prime}(f)$ becomes less than minus one, and the e,f cycle becomes unstable.

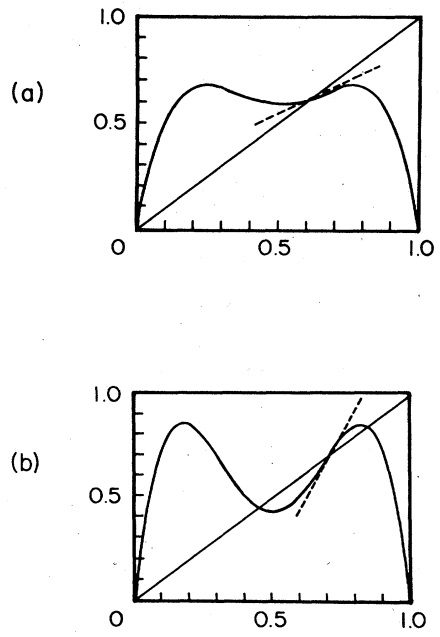

FIG. 5. x_{n+2} vs x_n for F_2 with (a) $b=0.678$ and (b) $b=0.854$. The dashed lines are the slope at $x=x^*$. The intersections of $x_{n+2}=x_n$ with $x_{n+2}=F_2^{(2)}(x_n)$ are $e>x^*>f$.

What happens next can be deduced, in an analogous way, from the map $x_{n+4}=F_2^{(2)}[F_2^{(2)}(x_n)]\equiv F_2^{(4)}(x_n)$. When the e,f cycle loses stability, a stable four-point periodic cycle simultaneously appears: $g,h,i,j,g,h,i,j,g,h,\ldots$, which then gives way ("bifurcates") to an eight-point cycle, which then gives way to a 16-point cycle, etc. Furthermore, the band of b values over which a given 2^k-point cycle is stable decreases geometrically with k, so that

$$\frac{b_k-b_{k-1}}{b_{k+1}-b_k}\to 4.669\,201\ldots \tag{2.6}$$

for $k\to\infty$, where b_k is the value of b at the point where the 2^k-point cycle bifurcates to a 2^{k+1}-point cycle. Also $b_k\to 0.892\ldots$ for $k\to\infty$; that is, there is an accumulation point of an infinite number of bifurcations at $b_\infty=0.892\ldots$. Fiegenbaum (1978) has derived Eq. (2.6) using arguments based on scale invariance near b_∞, and has also obtained other properties of the generated sequences for b near b_∞. These properties apply independently of the detailed functional form of the map as functional form of the map as long as it has a quadratic maximum as does F_2. Thus Eq. (2.6) applies to a wide class of maps.

Just past b the orbit generated by F_2 looks like a noisy cycle of periodicity 2^p with $p\to\infty$ as b approaches b_∞ from above. By a "noisy cycle of periodicity 2^p" we mean that the orbit is confined to 2^p disjoint intervals in $1>x>0$ which it visits in a sequential order. Thus the orbit always comes back to the same interval after 2^p iterations. On the other hand, if one looks at the points generated by $F_2^{(2^p)}$ with an initial condition in one of these intervals, then the orbit looks completely chaotic in this interval. As b increases, these intervals merge in pairs so that a noisy 2^p cycle goes into

a noisy 2^{p-1} cycle as b increases past a critical value $\bar{b}_p$. Furthermore, $\bar{b}_p$ obeys the same scaling relation[1] as in Eq. (2.6) (Coullet and Tresser, 1980). As b increases past $\bar{b}_1$, chaotic motion over a single connected band emerges.

In addition to the noisy 2^p cycles, narrow windows in b also exist within $b_\infty < b < 1.0$ for which the generated sequence is exactly periodic. Generally, these periodic sequences first appear with some period N and then go through a sequence of period doubling bifurcations, creating periods $2^k N$, with an accumulation point at $k \to \infty$ ending the particular periodic window. The widest such window is for 3×2^k periodic cycles, $0.9571 < b < 0.9624$. Other periodic windows are exceedingly narrow in b, and most of the range $b_\infty < b < 1$ appears to be chaotic. As an example of how these cycles first appear, consider the onset of the $N = 3$ period cycle. Figure 6 shows the map x_{n+3} versus x_n [obtained from $F_2^{(3)}(x_n)$] for values of b just below and just above that for which the $N = 3$ cycle first appears. As b increases past its critical value, the minimum of $F_2^{(3)}$ lowers until two new intersections of $F_2^{(3)}$ with $x_{n+3} = x_n$ are created near this minimum, one with slope greater than one (unstable) and one with slope less than one (initially stable). This type of phenomenon, whereby a periodic orbit appears after a region of chaotic motion, is called a *tangent bifurcation*. For values of b where numerically generated sequences appear to be chaotic, it is not, at present, known whether they are truly chaotic, or whether, in fact, they are really periodic, but with exceedingly large periods and very long transients required to settle down. Recent numerical results do, however, strongly suggest that the sequences are truly chaotic (Lorenz, 1979). Figure 7 summarizes some of the previously described results for F_2.

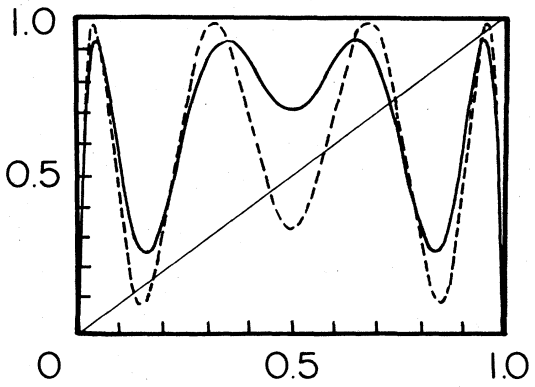

FIG. 6. x_{n+3} vs x_n for $b = 0.975$ (dashed curve) and for $b = 0.925$ (solid curve).

[1]The subject of the universal scaling properties of maps with a quadratic maximum is currently a very active research topic. Recent work includes the study of scaling of the Lyapunov number past b_∞ (Chang and Wright, 1981; Huberman and Rudnick, 1980), the noise power spectrum past b_∞ (Huberman and Zisook, 1981; Wolf and Swift, 1981), and scaling behavior with the addition of random noise (Crutchfield *et al.*, 1981; Shraiman *et al.*, 1981). Furthermore, universal scaling properties of conservative systems with period doubling have also recently been examined (for example, Green *et al.*, 1981).

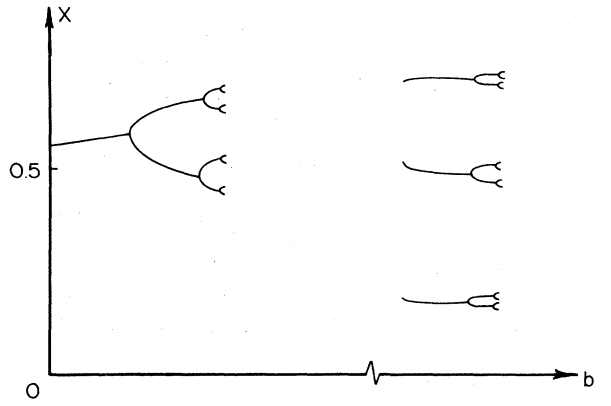

FIG. 7. Summary diagram for some of the bifurcations of $F^{(2)}$. The scale about the period 3×2^k cycles has been greatly expanded.

III. TWO-DIMENSIONAL INVERTIBLE MAPS

A general two-dimensional map can be written as

$$x_{n+1} = f_1(x_n, y_n), \quad y_{n+1} = f_2(x_n, y_n). \tag{3.1}$$

The map is invertible if (3.1) can be solved uniquely for x_n and y_n as functions of x_{n+1} and y_{n+1}, $x_n = g_1(x_{n+1}, y_{n+1})$ and $y_n = g_2(x_{n+1}, y_{n+1})$. That is, it is possible to go either backwards or forwards in time. A two-dimensional invertible map can easily be constructed from a one-dimensional noninvertible map as follows:

$$x_{n+1} = F(x_n) + y_n, \tag{3.2a}$$

$$y_{n+1} = \beta x_n, \tag{3.2b}$$

where $F(x)$ is noninvertible. For $\beta = 0$, $x_{n+1} = F(x_n)$, and the noninvertible one-dimensional map is recovered. However, as long as $\beta \neq 0$, no matter how small it is, the map (3.2) is invertible: $x_n = y_{n+1}/\beta$ and $y_n = x_{n+1} - F(y_{n+1}/\beta)$. On the other hand, if β is sufficiently small, the variation of x is well described by the one-dimensional map, $x_{n+1} = F(x_n)$. Furthermore, for small β, the range of variation of y_n will be small compared to that for x_n [cf. Eq. (3.2b)], and thus, if the points generated by (3.2) are plotted on the xy plane, the generated sequence will appear to lie on a line (the x axis) with some small spread about the line. For very small β, the spread may, in practical terms, be unmeasurable, so that (3.2) becomes indistinguishable from a one-dimensional noninvertible map. (This will, indeed, turn out to be similar to what happens in certain differential equation examples to be discussed in the next section.)

It is of interest to compute the Jacobian of the map (3.2),

$$J \equiv \begin{vmatrix} \frac{\partial x_{n+1}}{\partial x_n} & \frac{\partial x_{n+1}}{\partial y_n} \\ \frac{\partial y_{n+1}}{\partial x_n} & \frac{\partial y_{n+1}}{\partial y_n} \end{vmatrix} = -\beta.$$

Thus, for $|\beta| < 1$, we see that areas will contract by the factor $|\beta|$ on each application of the mapping (3.2). Thus, if the generated sequence of pairs (x_n, y_n) re-

mains in a bounded region of the xy plane, then the sequence must asymptotically approach a subset of the original bounded xy region which has zero area. This subset is called an *attractor*. For example, if the sequence becomes attracted to an N-point periodic cycle, then the attractor would be the N points plotted in the xy plane, clearly a subset of zero area. Another possible subset of zero area that a sequence might asymptote to is a curve. At first sight, these two possibilities, a zero-dimensional subset (points) and a one-dimensional subset (a curve), might appear to exhaust all possibilities for zero-area attractors. This is, however, not the case. There can be attractors which have noninteger dimension (at least according to the definition of dimension that we will use). Such attractors would be termed strange. The relevant definition of dimension is that due to Hausdorf[2] [see, for example, Mandelbrot (1977)]:

$$d=\lim_{\varepsilon\to 0}\ln N(\varepsilon)/\ln\left(\frac{1}{\varepsilon}\right), \tag{3.3}$$

where, if the set in question is a subset of a p-dimensional ordinary space, then $N(\varepsilon)$ is the number of p-dimensional cubes of side ε needed to cover the set. Alternatively, (3.3) implies that for small ε, $N(\varepsilon)\cong K\varepsilon^{-d}$. Thus, if one is content to know where the set lies to within an accuracy ε, then, to specify the location of the set, we need only specify the positions of the $N(\varepsilon)$ cubes covering the set. Hence, the dimension may be viewed as telling us how much information is necessary to specify the location of the set to within a given accuracy. If the set has complicated fine-scale structure, then, as a practical matter, it may be advantageous to introduce some coarse-graining into the description of the set, and then ε may be thought of as specifying the degree of coarse-graining. As an example of the application of Eq. (3.3), if the set in question is a point, then $N(\varepsilon)=1$, and, according to (3.3), the Hausdorf dimension is zero; if the set in question is the section of the xy plane given by $0<x<1$ and $0<y<1$, then $N(\varepsilon)=\varepsilon^{-2}$, and the Hausdorf dimension is two; if the set is a straight line joining (0, 0) and (1.0), then $N(\varepsilon)=\varepsilon^{-1}$, and the Hausdorf dimension is one. These examples all yield the obvious results, so that (3.3) conforms to our intuition in these cases. As an example of a set with a noninteger dimension, consider the following construction of a Cantor set (illustrated in Fig. 8): take a line of unit length, $0\leq x\leq 1$, and remove the middle third $\frac{1}{3}<x<\frac{2}{3}$; then take the two remaining intervals between 0 and $\frac{1}{3}$ and between $\frac{2}{3}$ and 1, divide them in thirds, and remove the two middle thirds; in the limit as this process is repeated an infinite number of times, what is left is a set that has zero net length and an uncountable number of elements. To apply (3.3) to this set, we note the following which is evident from Fig. 8,

$$\varepsilon=\tfrac{1}{3},\quad N=2$$

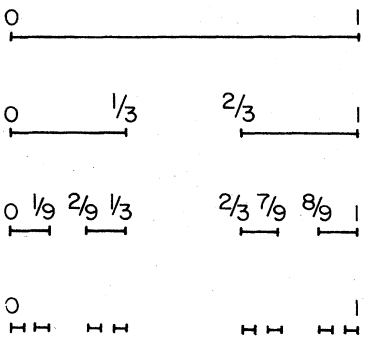

FIG. 8. First few steps in the construction of an example of a Cantor set.

$$\varepsilon=\tfrac{1}{9},\quad N=4$$

$$\varepsilon=\tfrac{1}{3}^{p},\quad N=2^{p}.$$

Thus from (3.3)

$$d=(\ln 2)/(\ln 3)=0.630.$$

Note that the Cantor set just constructed has the property of scale invariance. That is, by the nature of the construction, the set between 0 and 1 will look precisely the same as that part of it between 0 and $\frac{1}{3}$, if the latter is examined under a magnifying glass which magnifies by a factor of three.

As a concrete example, we now consider a mapping first studied by Henon (1976):

$$x_{n+1}=1-cx_n^2+y_n,\quad y_{n+1}=\beta x_n. \tag{3.4}$$

This mapping is essentially equivalent to Eq. (3.2) with F given by Eq. (2.3). [A study of the map obtained from (3.2) and (2.2) has been presented by Lozi (1978), but will not be discussed here.] Figure 9 shows the results of plotting 10^4 successive points obtained by iterating the map (3.4) with $c=1.4$ and $\beta=0.3$ from an initial point $x_0=0.631$, $y_0=0.189$. Similarly obtained

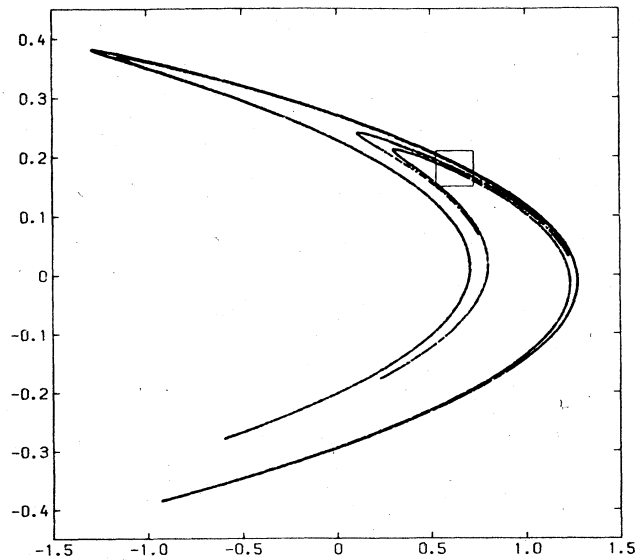

FIG. 9. Iterated points of the map, Eq. (3.4), 10^4 iterations.

[2]Actually, the Hausdorf dimension has a somewhat more involved definition than that given by Eq. (3.3). More precisely, d given by (3.3) defines the "capacity" of the set. For cases of interest to us here, however, Eq. (3.3) probably gives the same result as would the actual Hausdorf dimension definition.

plots starting with other initial values are almost identical (except for an initial transient), suggesting that Fig. 9 is, in fact, essentially a picture of the attractor. That is, as the map is iterated, points come closer and closer to the attractor and eventually become indistinguishable from it on the scale of the figure. Figure 10(a) shows a blow-up of the squared region in Fig. 9; Figs. 10(b) and 10(c) are successive blow-ups of the squared regions in the preceding figure. Scale invariant, Cantor-set-like structure transverse to the linear structure is evident. Thus, the attractor is probably strange with dimension between one and two. In fact, a recent study (Russell *et al.*, 1980) gives $d \cong 1.26$. Further studies of the map (3.4) have been carried out by Feit (1978), Curry (1979), and Simó (1979), who have explicitly verified exponential divergence of initially close points. In addition, Feit (1978) and Simó (1979) have studied how the character of the generated sequences changes as c is varied with β fixed. It is found that, dispersed among intervals of c where the motion is chaotic, there are many small subintervals where the motion is periodic. On each such subinterval, there appear attractors of period $k, 2k, 4k, \ldots, 2^n k, \ldots$, similar to the phenomenon observed for the one-dimensional map, Eq. (3.4) with $\beta = 0$ [which is equivalent to Eq. (2.3)].

Bridges and Rowlands (1977) have given a procedure for investigating maps of the type (3.2) essentially by a power series in β. For example, to lowest order in β (3.2a) gives $x_{n+1} = F(x_n)$ (as previously noted), which, when substituted into (3.2b), yields the result that the attractor lies in the vicinity of the curve

$$x = F(y/\beta). \tag{3.5}$$

Higher-order approximations yield increasing detail to the curve. For Henon's map, Eq. (3.4), with $c = 1.4$ and $\beta = 0.3$, Eq. (3.5) yields a surprisingly good first-order approximation of the attractor.

The reader may be aware that two-dimensional maps have been extensively utilized as models of Hamiltonian systems, and, in particular, to model ergodic behavior in Hamiltonian systems. Since Hamilton's equations conserve phase-space volume (by Liouville's theorem), two-dimensional maps modeling Hamiltonian systems do not cause uniform contraction of areas, and chaotic motions (i.e., ergodicity) generated by such maps generally fill up a two-dimensional area. Thus, no strange (fractional dimensional) set is involved. If dissipation (e.g., friction) is added to a Hamiltonian system, phase-space contraction may be expected to result. Thus it is of interest to consider the relation of ergodicity in Hamiltonian systems to the possible

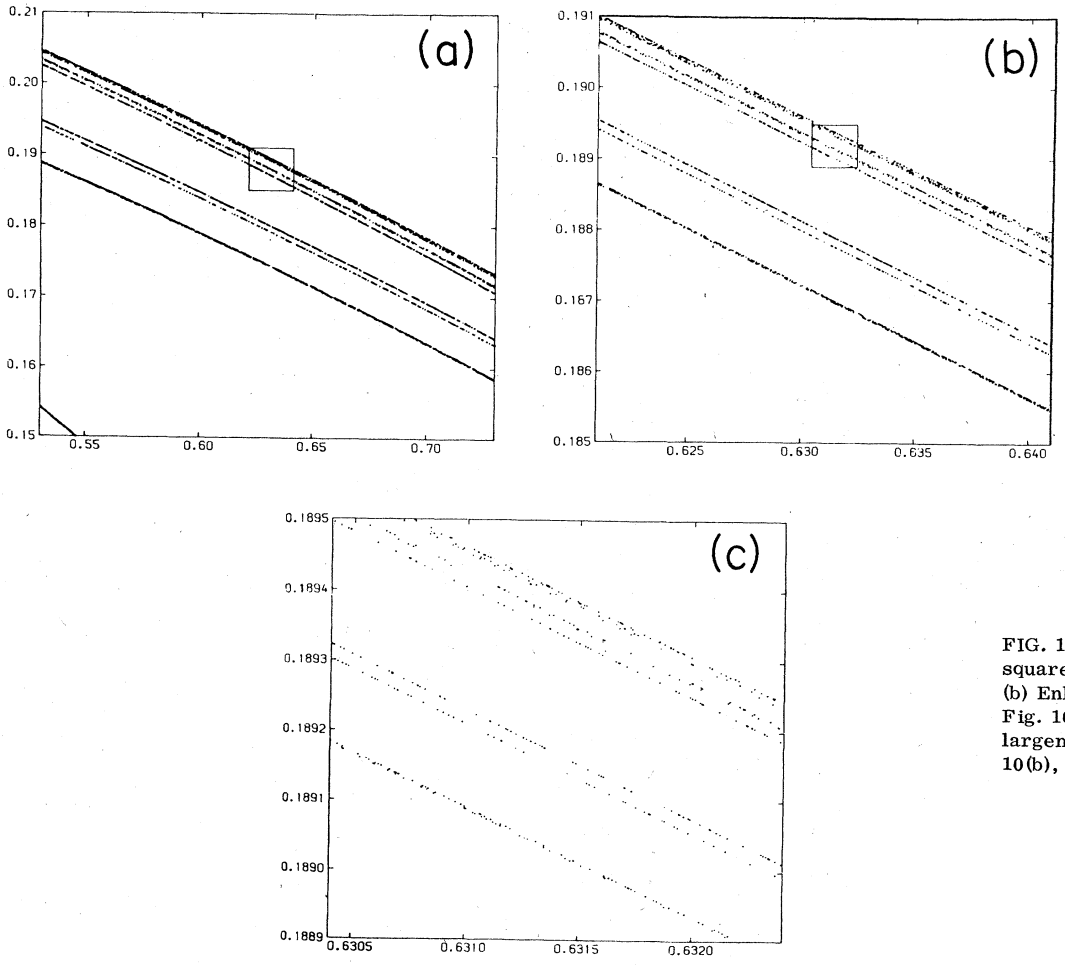

FIG. 10. (a) Enlargement of the square in Fig. 9, 10^5 iterations; (b) Enlargement of the square in Fig. 10(a), 10^6 iterations; (c) Enlargement of the square in Fig. 10(b), 5×10^6 iterations.

appearance of strange attractors when dissipation is added to these systems (McLaughlin, 1979; Zaslavskii, 1978). Recent studies addressed to this question (Zaslavskii, 1978; Zaslavskii and Rachko, 1979) consider the two-dimensional map

$$y_{n+1} = e^{-\Gamma}(y_n + \varepsilon \cos 2\pi x_n), \tag{3.6a}$$

$$x_{n+1} = \left\langle x_n + \frac{\Omega}{2\pi} + \frac{\alpha\Omega}{2\pi\Gamma}(1-e^{-\Gamma})y_n + \frac{K}{\Gamma}(1-e^{-\Gamma})\cos 2\pi x_n \right\rangle, \tag{3.6b}$$

where $\langle \cdots \rangle$ denotes the fractional part of the argument and $K = \alpha\varepsilon\Omega/2\pi$. The Jacobian of the map (3.6) is $\exp(-\Gamma)$. Thus, the map contracts areas for $\Gamma > 0$ and is area preserving for $\Gamma = 0$. In the absence of dissipation, $\Gamma = 0$, and (3.6) reduces to

$$y_{n+1} = y_n + \varepsilon \cos 2\pi x_n, \tag{3.7a}$$

$$x_{n+1} = \left\langle x_n + \frac{\Omega}{2\pi} + \frac{\alpha\Omega}{2\pi} y_n + K \cos 2\pi x_n \right\rangle, \tag{3.7b}$$

which has been extensively studied as a basic model of stochasticity in Hamiltonian systems (Rosenbluth *et al.*, 1966; Stix, 1973; Rechester and Stix, 1976; Chirikov, 1979; Greene, 1979) (and also as a model for stochastic magnetic field line topologies in magnetic confinement controlled thermonuclear fusion devices). The onset of ergodic behavior in the map (3.7) can be estimated from Chirikov's island overlap condition which, for small ε, yields ergodicity for $K \simeq 1$. By qualitative arguments based upon the exponential divergence of nearby chaotic orbits Zaslavskii is able to estimate the condition for the appearance of chaotic orbits and a strange attractor for the map (3.6), $K\mu \gtrsim 1$, where $\mu = (1-e^{-\Gamma})\Gamma^{-1}$. Numerical results confirm this rough estimate.

In connection with chaotic maps a useful notion is that of the Lyapunov numbers. An illustration of the Lyapunov numbers is given in Fig. 11. For a two-dimensional map, the Lyapunov numbers, λ_1 and λ_2, are the average principal stretching factors for a very small circular area; more formally

$$(\lambda_1, \lambda_2) = \lim_{n\to\infty} [\text{magnitude of the eigenvalues of } \underline{J}(x_n, y_n)\underline{J}(x_{n-1}, y_{n-1})\cdots\underline{J}(x_1, y_1)]^{1/n}, \tag{3.8}$$

where $\underline{J}(x,y)$ is the Jacobian matrix of the map:

$$\underline{J}(x,y) = \begin{bmatrix} \frac{\partial f_1(x,y)}{\partial x} & \frac{\partial f_1(x,y)}{\partial y} \\ \frac{\partial f_2(x,y)}{\partial x} & \frac{\partial f_2(x,y)}{\partial y} \end{bmatrix}$$

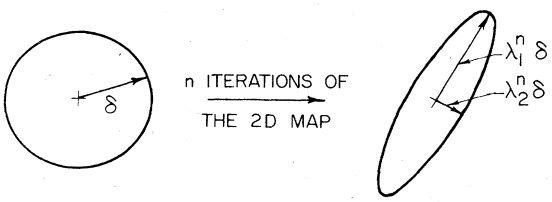

FIG. 11. n iterations of the two-dimensional map transform a sufficiently small circle of radius δ approximately into an ellipse with major and minor radii $\lambda_1^n\delta$ and $\lambda_2^n\delta$, where λ_1 and λ_2 are Lyapunov numbers, for $n \to \infty$.

[f_1 and f_2 are defined by Eq. (2.2)], and (x_1, y_1), (x_2, y_2), $\ldots, (x_n, y_n)$ is a sequence generated by the map. Thus, the Lyapunov numbers specify the average stretching rate of nearby points. Say $\lambda_1 > \lambda_2$. If the map is chaotic, then λ_1 must exceed unity, so that the distance between almost all nearby points increases on successive mappings. If the map is area contracting, $\lambda_1\lambda_2 < 1$; if it is area preserving, $\lambda_1\lambda_2 = 1$. The calculation of λ_1 and λ_2 from Eq. (3.8) is fairly easy using a digital computer and can then be used as a criterion for chaos, $\lambda_1 > 1$. An interesting conjecture concerning Lyapunov numbers has been put forward by Frederickson *et al.* (1980) [see also Kaplan and Yorke (1979a)], namely, that the Hausdorf dimension of a strange attractor of a map with the eigenvalues of $\underline{J}$ independent of x and y is related to its Lyapunov numbers. For a two-dimensional map with Lyapunov numbers $\lambda_1 > 1 > \lambda_2$, $\lambda_1\lambda_2 < 1$, their conjecture states that the dimension is given by

$$d = 1 + (\ln\lambda_1)/(\ln\lambda_2^{-1}). \tag{3.9}$$

For example, for the Henon map, Eq. (3.4), with $c = 1.4$ and $b = 0.3$, $\lambda_1 \cong 0.2$, and Eq. (3.9) gives $d \cong 1.26$. Recently, numerical experiments have been performed which tend to confirm (3.9) (Russell *et al.*, 1980). Furthermore, we note that these numerical experiments also tested maps for which the eigenvalues $\underline{J}$ are not independent of x and y and still obtained excellent agreement with Eq. (3.9). While it is known by counterexample that Eq. (3.9) fails in general if the eigenvalues of $\underline{J}$ depend on x and y, the results of these computer experiments indicate that (3.9) still yields a surprisingly good approximation to the dimension in some cases.

A possible motivation for (3.9) is depicted in Fig. 12, which considers a map of the unit square into itself. The mapping consists of two steps. The first step is a stretching along y by $\lambda_1 > 1$ and a contraction along x by $\lambda_2 < 1$. For the second step, we assume that λ_1 is an integer ($\lambda_1 = 3$ for Fig. 12), and move the stretched and contracted area back into the unit square, as shown. This may be represented analytically by the map

$$y_{n+1} = \lambda_1 y_n \bmod 1,$$

$$x_{n+1} = \lambda_2 x_n + y_n - \lambda_1^{-1}(\lambda_1 y_n \bmod 1).$$

From the construction in Fig. 12, it is clear that λ_1 and λ_2 are the Lyapunov numbers of this map. If the proc-

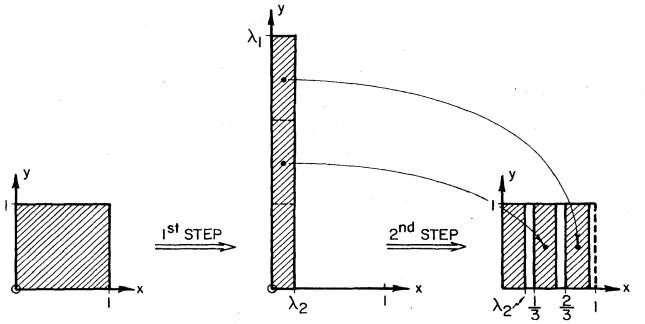

FIG. 12. Map motivating Eq. (3.9). The illustrated map may be represented analytically as $y_{n+1} = 3y_n \bmod 1$, $x_{n+1} = \lambda_2 x_n + y_n - y_{n+1}/3$.

ess in Fig. 12 is repeated p times, λ_1^p vertical strips of width λ_2^p will be created. To apply Eq. (3.3) for the dimension, let $\varepsilon = \lambda_2^p$. Then, the number of squares of side ε needed to cover the strips is $N \cong \lambda_1^p \lambda_2^{-p}$, and Eq. (3.3) yields (3.9). In addition, the conjecture can be used to predict the dimension of strange attractors for systems of ordinary differential equations (Russell *et al.*, 1980). The map of Fig. 12 is also interesting, since it demonstrably yields a strange attractor, while for maps such as (3.4) and (3.6) one can only say that numerical results suggest the presence of a strange attractor.

IV. THREE-DIMENSIONAL SYSTEMS OF ORDINARY DIFFERENTIAL EQUATIONS

A. Background

Here we consider systems of three coupled, nonlinear, autonomous, differential equations,

$$dx_i(t)/dt = f_i[x_1(t), x_2(t), x_3(t)], \quad i = 1, 2, 3. \tag{4.1}$$

The system is "autonomous" because f_i does not depend explicitly on t but only on x_i. Alternatively, a nonautonomous system of two coupled equations, $dx_1/dt = g_1(x_1, x_2, t)$ and $dx_2/dt = g_2(x_1, x_2, t)$, can be written in the form (4.1) by defining $f_1 = g_1(x_1, x_2, x_3)$; $f_2 = g_2(x_1, x_2, x_3)$; $f_3 = 1$.

We now define the Poincaré map of a system like (4.1). The Poincaré map represents a reduction of a system like (4.1) to a two-dimensional map, such as those studied in Sec. III. Figure 13 illustrates the construction of a Poincaré map. Consider a particular solution of (4.1) to generate an orbit in x_1, x_2, x_3 phase space. We now assume that some appropriate surface (the "surface of section") in this space has been chosen, and we study intersections of the orbit with the chosen surface. In Fig. 13 the chosen surface is the plane $x_2 = K$. Every time the orbit crosses the chosen surface in a particular direction ($dx_2/dt < 0$ for Fig. 13) we record the crossing point, e.g., points A and B in Fig. 13. For Fig. 13, it is clear that point A uniquely determines point B, since the solution of (4.1) is unique. Likewise, point B determines point A by time reversal of (4.1). Thus the Poincaré map in this illustration represents an invertible transformation of a point in the plane $x_2 = K$ into another point, i.e., it is an invertible two-dimensional map.

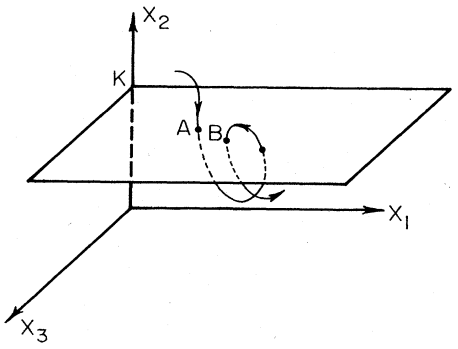

FIG. 13. Poincaré map of Eq. (4.1).

As an example, we consider the following system of two nonautonomous ordinary differential equations:

$$\frac{dp}{dt} = f(q) \sum_{n=-\infty}^{+\infty} \delta(\omega t - 2n\pi) - \nu(p - p_0),$$

$$\frac{dq}{dt} = p,$$

where $\delta(\theta)$ denotes the delta function of θ. This can be written as three autonomous equations

$$\frac{dp}{dt} = f(q) \sum_{n=-\infty}^{+\infty} \delta(\theta - 2n\pi) - \nu(p - p_0), \tag{4.2a}$$

$$\frac{dq}{dt} = p, \tag{4.2b}$$

$$\frac{d\theta}{dt} = \omega. \tag{4.2c}$$

We take the surface of section to be $\theta = 2m\pi - \varepsilon$, where $\varepsilon \to 0^+$. Defining $(p_m, q_m) = \lim_{\epsilon \to 0^+}[p(t_m - \varepsilon), q(t_m - \varepsilon)]$, and $t_m = 2m\pi/\omega$, Eqs. (4.2) then yield by simple integration, the following two-dimensional map:

$$y_{m+1} = e^{-\Gamma}[y_m + f(q_m)] \tag{4.3a}$$

$$q_{m+1} = q_m + (1 - e^{-\Gamma})\nu^{-1}[y_m + f(q_m)] + 2\pi p_0/\omega, \tag{4.3b}$$

where $\Gamma = 2\pi\nu/\omega$, and $y_m = p_m - p_0$. By a suitable choice of $f(q)$ this two-dimensional map may be reduced to that studied by Zaslavskii (1978) and discussed in the preceding section.

Now, we turn to a discussion of the evolution of phase-space volumes as governed by the system (4.1). That is, we consider the volume (V) enclosed by some closed surface S in the x_1, x_2, x_3 phase space, and let the surface evolve by having each point on the surface follow an orbit generated by (4.1). By the divergence theorem

$$\frac{dV}{dt} = \int_V \left(\sum_{i=1}^{3} \frac{\partial f_i}{\partial x_i} \right) dx_1 dx_2 dx_3. \tag{4.4}$$

In the special case where divergence of the phase-space flow, $\sum_{i=1}^{3} \partial f_i/\partial x_i$, is a negative constant, $\sum_{i=1}^{3} \partial f_i/\partial x_i = -k$, Eq. (4.4) yields $dV/dt = -kV$, so that

$$V(t) = V(0) \exp(-kt). \tag{4.5}$$

Thus phase-space volumes shrink exponentially in time. Many of the physical examples yielding a system of the form (4.1) that have been investigated for strange attractors also happen to have a constant negative divergence. We shall restrict our discussion in the remainder of this section to this case. [In fact, Eqs. (4.2) fall in this class with the flow divergence being $-\nu$.] In Sec. V, more general cases, without negative divergence, will be discussed.

The special case of three ordinary autonomous differential equations with negative phase-space flow divergence presents a very clear case for the necessity of introducing the concept of a strange attractor. Since phase-space volume contracts to zero in the limit of large time, it follows that any attractor must have zero volume. A natural assumption might then be that the attractor would have to be a surface (two dimensional), a curve (one dimensional), or a point (zero dimension-

al). However, none of these allows chaotic motion. In particular, not even the highest dimension of the above three possibilities (two) allows chaos. For example, for orbits within a finite section of a plane, the Poincaré-Bendixson theorem shows that the only possible attractor for the orbit must be either a point, a simple closed curve, or a self-intersecting closed curve[3] (e.g., a figure eight (e.g., Hirsch and Smale, 1974). Thus if one observes chaotic motion in the system (4.1), and if (4.1) has negative phase-space flow divergence, then one is faced with something of a paradox. One way out is to realize that attractors with zero volume need not only have dimension zero, one, or two, but can, in fact, have noninteger dimension. In particular, chaotic motion is possible if Eqs. (4.1) have an attractor of dimension greater than two but less than three (the latter so that the volume of the attractor is zero), i.e., a strange attractor. We will now outline some work on physically interesting systems exhibiting strange attractors. The three examples which we will discuss are (1) the so-called Lorentz system, which represents a simple model of the convective motions that result when a temperature difference is maintained across a fluid layer which is subjected to gravity, (2) a simple model for the saturation of an unstable mode by coupling energy through quadratic nonlinearities from the unstable mode to damped modes, and (3) a model similar to (2) but with cubic nonlinearities (resulting, for example, from a nonlinear Schrödinger equation).

B. Examples

The first two examples, (1) and (2), are for parameters such that the phase-space contraction rate is large. This has the consequence that the attractor in the surface of section appears to be one dimensional. Actually, closer examination under magnification would reveal thickness containing structure within the attractor. Furthermore, the dimension in the surface of section must be $1<d<2$, as for any invertible two-dimensional map with a strange attractor. Here, however, d is only slightly larger than one. This leads to the result that the system dynamics can be well approximated by a one-dimensional noninvertible map of the types discussed in Sec. II. [Recall that, as discussed in Sec. III, this also is true in the analogous case of the two-dimensional map, Eq. (3.2) with β small.] The example in (1) yields a one-dimensional map that is like that given by Eq. (2.2); it has a sharp (nondifferentiable) maximum, and, in the notation of Sec. II, $|F'(x)|>1$ for all points on the chaotic orbit generated by $x_{n+1}=F(x_n)$. The example in (2) yields a one-dimensional map that is like that given in Eq. (2.3). As a consequence, example (2) leads to a pattern of period doubling bifurcations, tangent bifurcations, and chaotic orbits that is essentially the same as that for the quadratic map, Eq. (2.3) (cf. Fig. 7). Example (3) will be discussed for a range of parameters for which the contraction rate is not large. Thus, for example (3), non-one-dimensional structure will be readily evident in the surface of section. Furthermore, it will be shown that this structure appears to have approximate scale-invariant properties upon magnification, in analogy to the Cantor set example of Sec. III (cf. Fig. 8) and to the Henon map (cf. Figs. 9 and 10). Thus these three examples serve to illustrate the relevance of essential features of one- and two-dimensional chaotic maps to systems of ordinary differential equations modeling physical systems.

1. Lorenz's treatment of the Benard instability

Consider two rigid plane parallel walls at $z=0, L$ with a fluid occupying the space in between. Gravity is in the negative z direction, and the plate at $z=0$ is maintained at a higher temperature than the plate at $z=L$, $T_0>T_L$. A possible equilibrium of this system is one in which the fluid is at rest and heat is transported from $z=0$ to $z=L$ via thermal conduction. Lord Rayleigh studied the linear stability of this equilibrium and found that if (T_0-T_L) exceeds a critical value, then the system becomes unstable to perturbations in the form of circulating fluid flow. The linear analysis cannot, however, be used to specify the ultimate nonlinear state of the fluid once instability sets in. Considering variations only in two dimensions, Saltzman (1962) derived a set of nonlinear ordinary differential equations by expanding the stream function and the temperature perturbation in double spatial Fourier series, with coefficients functions of t alone. By substituting the series into the original governing set of partial differential equations and truncating the infinite sum to a finite number of terms, he obtained a set of ordinary differential equations. Lorenz (1963) further examined this problem and added much insight. The paper by Lorenz has greatly added to the understanding of this type of problem. Lorenz considered a truncation to only three Fourier modes, for which the describing equations become

$$dX/dt=-\sigma X+\sigma Y\,, \tag{4.6a}$$

$$dY/dt=-XZ+rX-Y\,, \tag{4.6b}$$

$$dZ/dt=XY-bZ\,, \tag{4.6c}$$

where σ, r, and b are dimensionless parameters of the system. X is proportional to the circulatory fluid flow velocity, Y characterizes the temperature difference between ascending and descending fluid elements, and Z is proportional to the distortion of the vertical temperature profile from its equilibrium (which is linear with height).

Setting $dX/dt=dY/dt=dZ/dt=0$, we find that (4.6) possesses steady-state solutions, $X=Y=Z=0$, and if $r>1$,

[3]For motion described by more than three autonomous ordinary differential equations with phase-space contraction, $\sum_i \partial f_i/\partial x_i<0$, or by three autonomous equations where $\sum \partial f_i/\partial x_i$ is not everywhere negative, an attractor which is a toroidal surface is possible. Motion on the toroidal surface is doubly periodic; that is, the solution of (4.1) can be represented as $x_i(t)=l_i(t,t)$, where l_i is periodic in both variables, $l_i(t+T_i,t+T_2)=l_i(t,t)$, and T_1/T_2 is not a rational number. Alternatively, if the orbit is doubly periodic, then the only frequency components of the Fourier spectrum of $x_i(t)$ are $(m/T_1)+(n/T_2)$, where m and n are integers. Doubly periodic motion in three dimensions with phase-space contraction is not possible, because the volume V enclosed by the toroidal attractor would be time independent, contrary to Eq. (4.5). At any rate, doubly periodic orbits are not chaotic, either.

$X = Y = \pm[b(r-1)]^{1/2}$, $Z = r - 1$. The equilibrium $X = Y = Z = 0$ represents the case of no fluid flow, while the two possible equilibria for $r > 1$ represent steady circulating convection. Linearization of Eqs. (4.6) about these equilibria reveals that the $X = Y = Z = 0$ equilibrium looses stability when $r > 1$, while the steadily convecting equilibria become unstable if

$$r > \sigma(\sigma + b + 3)(\sigma - b - 1) \equiv r_c \tag{4.7}$$

and $\sigma > b + 1$.

Lorenz numerically considered the solution of (4.6) for a case in which (4.7) is satisfied: $\sigma = 10$, $b = \frac{8}{3}$, $r = 28$. [Note that from (4.7) $r_c = 24.74$ in this case.] For these values of the parameters he obtained a chaotic solution and examined its properties in detail. It is instructive also briefly to consider the character of the solutions of (4.6) for other parameters. In particular, say $\sigma = 10$, $b = \frac{8}{3}$, and increase r. For $r < 1$ all initial conditions eventually decay to the convection-free equilibrium. For $1 < r \lesssim 24.06$ all initial conditions eventually settle into one of the two stable convective equilibria. For $24.07 \lesssim r \lesssim 24.74$, depending on initial conditions, the solution settles into either a chaotic motion or into one of the two stable convective equilibria. This phenomenon of dependence upon initial conditions is called hysteresis. For $r > 24.74$ the eventual orbit is chaotic for all initial conditions. [For r still larger, say $r \gtrsim 50$, the behavior can again change (Shimzu and Morioda, 1978).] Even in the range $r < 24.06$ interesting behavior arises, in particular, the phenomenon of "chaotic transients" first noted by Yorke and Yorke (1979) and by Kaplan and Yorke (1979b). These authors find that the evolution from a given initial condition initially looks very much like the time dependence of the solution in the chaotic regime, after which the solution quickly settles into one of the two stable equilibria. Furthermore, they find that the time to settle into equilibrium is sensitive to the initial condition, and can be fairly long with its duration increasing with r. Similar phenomena are to be expected in other cases (e.g., Shimzu and Morioda, 1978) and in other systems.

We now return to a description of Lorenz's results for $r = 28$. Figure 14 shows a projection of the phase-space orbit of the system onto the YZ plane. The points labeled C and C' are the steady convection equilibria points. Evidently, the orbit spirals outward

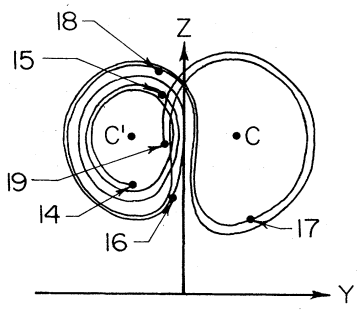

FIG. 14. Projections of an orbit for $r = 28$ onto the YZ plane. Numerals 14, 15, etc., denote positions at iterations 1400, 1500, etc.

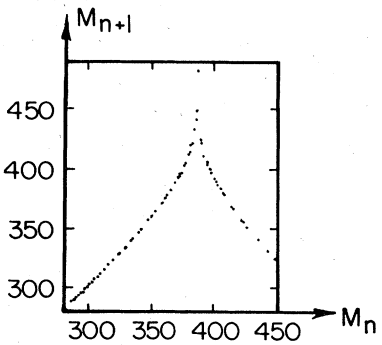

FIG. 15. Maxima vs subsequent maxima of Z occurring during 6000 iterations.

from one of the points C or C' until it exceeds some critical distance from the origin, at which point it starts spiraling about the other point. If one were to make a sequential list of the number of circuits the solution makes around one point before it switches to the other point, the sequence would appear to be chaotic. By examination of the solution, Lorenz has deduced that the orbit appears to be confined to a surface. Actually this apparent "surface" must have some small thickness, inside of which is embedded the more complicated structure of the strange attractor. In fact, if one were to pass a line through this surface normal to it, one would find that the intersection of the line with the surface is a set of dimension $0 < d < 1$, i.e., like the Cantor set of Fig. 8. However, since the thickness of the strange attractor is small, the presence of structure in this intersection would only be visible upon magnification, and, unmagnified, it would appear to be a point.

Figure 15 shows a plot, obtained by Lorenz, of M_n, the nth maximum of Z, versus M_{n+1}, the value of the following maximum. It is clear that an (approximate) one-dimensional map is generated. Furthermore, $|dM_{n+1}/dM_n| > 1$, which is similar to the result for Eq. (2.2) with $a > \frac{1}{2}$. Thus, as for Eq. (2.2), we expect this one-dimensional map to generate a chaotic sequence. For later comparison with the results of example (2), note that the maxima of Z may be regarded to lie in a surface of section, $bZ = XY$ [put $dZ/dt = 0$ in (4.6c)]. For further discussion of the Lorenz attractor see Lanford (1976), Afraymovich *et al.* (1977), and Bunimovich and Sinai (1977).

2. Instability saturation by quadratically nonlinear mode coupling

An important problem in plasma physics (and in other fields as well) is that of determining the nonlinear state resulting from a linearly unstable wave. An elementary process by which saturation can occur is that of resonant three-wave mode coupling of energy in the linearly unstable wave to two other waves which are linearly damped. The following normalized system of equations describes this process:

$$dC_1/dt = C_1 + C_2 C_3 \exp(i\delta t),$$

$$dC_{2,3}/dt = -\gamma_{2,3} C_{2,3} - C_1 C^*_{3,2} \exp(i\delta t),$$

where C_i ($i=1,2,3$) are time-dependent complex wave amplitudes, C_i^* is the complex conjugate of C_i, times have been normalized to the growth rate of wave 1 (the higher frequency wave), δ represents the effect of a mismatch in the frequency resonance, and amplitudes have been normalized so that the coefficients of the nonlinear terms are one. Introducing $a_1\exp(i\phi_1)=C_1$, $a_{2,3}\exp(i\phi_{2,3})=C_{2,3}\exp(i\delta t/2)$, and $\phi=\phi_1-\phi_2-\phi_3$, where a_i and ϕ_i are real, the previous system gives four real equations for $a_{1,2,3}$ and ϕ. These equations readily yield

$$d(a_2^2-a_3^2)/dt=-2(\gamma_2 a_2^2-\gamma_3 a_3^2).$$

Thus in the special case $\gamma_2=\gamma_3$, $a_2^2-a_3^2$ decreases exponentially. Restricting consideration to $\gamma_2=\gamma_3\equiv\gamma$ and $a_2=a_3$, the basic equations then become (Vyshkind and Rabinovich, 1976)

$$da_1/dt=a_1+a_2^2\cos\phi\,,$$
$$da_2/dt=-a_2(\gamma+a_1\cos\phi)\,,$$
$$d\phi/dt=-\delta+a_1^{-1}(2a_1^2-a_2^2)\sin\phi\,.$$

For definiteness in examining this system, Wersinger *et al.* (1980a, 1980b, 1980c) chose $\delta=2$ and studied the properties of numerical solutions[4] for a range of γ from $\gamma=1$ to $\gamma=25$. For $\gamma\lesssim 3$ the damping was not strong enough to arrest the instability, and the system evolution was apparently unbounded. For $3\lesssim\gamma\lesssim 8.5$, all initial conditions led to a simple periodic limit cycle. Using $\phi(t)=\pi/2$ as the surface of section, this limit cycle was manifested as a single point in the surface of section. For γ somewhat larger than 8.5 a limit cycle is still observed, but the single fixed point in the surface of section that previously manifested the limit cycle splits into two points that are visited alternately. Correspondingly, the single-peak-per-period function for $3\lesssim\gamma\lesssim 8.5$ becomes a function with two alternating maxima (cf. Figs. 16 and 17). As γ is increased, the two-point cycle splits into a four-point cycle (for $\gamma\gtrsim 11.9$), which splits into an eight-point cycle (for $\gamma\cong 13.15$), ..., followed by a region of γ ($\gamma\lesssim 13.4$) for

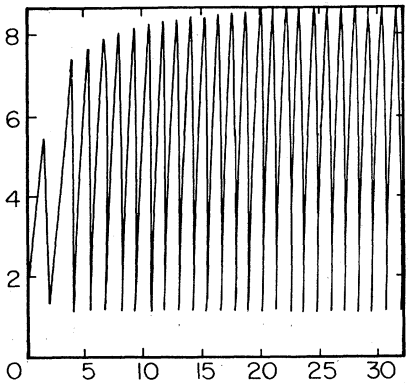

FIG. 16. a_1 vs t for $\gamma=3$. After an initial transient, the solution settles into a limit cycle.

[4]For larger values of δ time-independent equilibrium solutions of the equations exist.

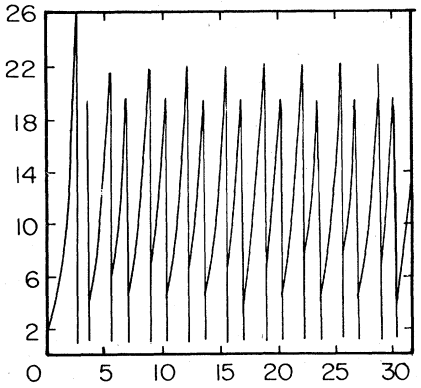

FIG. 17. a_1 vs t for $\gamma=9$.

which the generated sequence appears chaotic[5] (cf. Fig. 18). For still larger γ a sequence from a three-point cycle to a six-point cycle, etc., briefly appears. To summarize, the phenomenology is precisely the same as that depicted in Fig. 7 for the one-dimensional quadratic map,[6] Eq. (2.3)! Similar results for entirely different physical situations have also been obtained [see, for example, Tomita and Kai (1979)]. To make the correspondence with Eq. (2.3) more concrete, first consider results from the numerically generated surface of section shown in Fig. 19 for a value of γ in the chaotic regime, $\gamma=15$. It is seen that the points generated in the surface of section *appear* to lie on an arc. Since this arc has no visible thickness, it is natural to attempt an approximate reduction to a one-dimensional map. This can be done, for example, by plotting $x_{n+1}\equiv a_2(t_{n+1})$ versus $x_n\equiv a_2(t_n)$, where t_n is the nth time at which the system orbit pierces the surface of section. The points so generated (cf. Fig. 20) lie along a curve $x_{n+1}=F(x_n)$. By a change of variables (e.g., $\bar{x}_n\equiv(\text{const})-x_n$) the one-dimensional map in Fig. 20 can be turned upside down so that it has a smooth rounded maximum (rather than

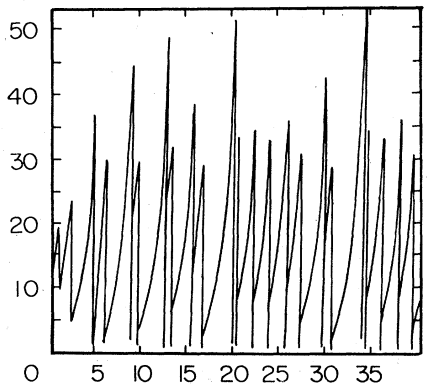

FIG. 18. a_1 vs t for $\gamma=15$.

[5]Feigenbaum (1979) has shown that the frequency power spectrum at the accumulation point of the period doubling bifurcations of a differential equation system has universal properties.

[6]This includes the phenomenon of noisy 2^p cycles studied by Crutchfield *et al.* (1980) by computations on another set of differential equations.

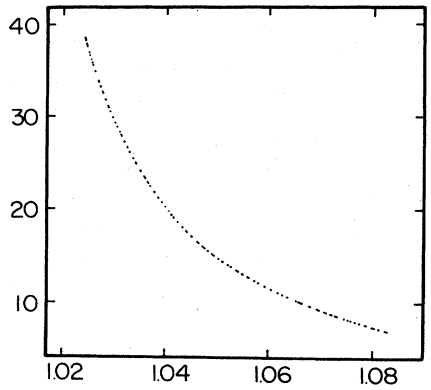

FIG. 19. Surface of section for $\gamma = 15$.

minimum). Thus we see that the one-dimensional map generated by the particular system discussed is of the same general character as the simple quadratic map discussed in Sec. II, Eq. (2.3), i.e., it is concave down with a smooth rounded maximum.

3. Instability saturation by cubicly nonlinear mode coupling

Here we very briefly describe another study of nonlinear mode coupling saturation of an unstable plasma wave. The physical situation, however, is somewhat different from that considered in example (2) in that a resonant three-wave process is precluded by the wave dispersion relation. The physical system is assumed to be well modeled by the following normalized, one-dimensional, nonlinear Schrödinger equation with linear wave growth and damping included,

$$i\left(\frac{\partial E}{\partial t}+\hat{\gamma}E\right)+\frac{\partial^2 E}{\partial x^2}+[\,|E|^2-|E|_0^2]E=0\,,$$

where E is the complex amplitude coefficient of the x-directed electric field, $|E|_0^2$ denotes the spatial average of $|E|^2$, and $\hat{\gamma}$ is a linear growth-damping operator defined so that the Fourier transform of $\hat{\gamma}E(x,t)$ is $\gamma(k)E_k(t)$ with $E_k(t)$ the Fourier coefficient of E and $\gamma(k)$ the linear damping rate of a wave of wave number k [$\gamma(k)<0$ for growth]. This equation may be used to model a situation where an electron beam with a thermal spread is injected into a plasma [cf. Russell and Ott (1980) and references therein]. Under suitable conditions on $\gamma(k)$ it is possible to consider $E(x,t)$ to consist of just three wave number components, k_0, k_1, k_2, with $2k_0 = k_1 + k_2$. There then results a system of ordinary differential equations for the three complex wave amplitudes corresponding to the three wave numbers,

$$\frac{dE_0}{dt}=-\gamma(k_0)E_0+i[\,|E_1|^2E_0+|E_2|^2E_0+2E_0^*E_1E_2\exp(2i\delta t)]\,,$$

$$\frac{dE_1}{dt}=-\gamma(k_1)E_1+i[\,|E_0|^2E_1+|E_2|^2E_1+E_0^2E_2^*\exp(-2i\delta t)]\,,$$

$$\frac{dE_2}{dt}=-\gamma(k_2)E_2+i[\,|E_0|^2E_2+|E_1|^2E_2+E_0^2E_1^*\exp(-2i\delta t)]\,,$$

where we assume $\gamma(k_0)<0$ and $\gamma(k_{1,2})>0$. As in example (2), if $\gamma(k_1)=\gamma(k_2)$, these three complex equations can be reduced to a system of three real equations:

$$\frac{da_0}{dt}=a_0+2a_0a_1^2\sin\phi\,,$$

$$\frac{da_1}{dt}=-\gamma a_1-a_0^2a_1\sin\phi\,,$$

$$\frac{d\phi}{dt}=-2\delta+2(a_1^2-a_0^2)+2(2a_1^2-a_0^2)\cos\phi\,.$$

The above system has been examined analytically and numerically as a function of the dimensionless parameters of the system (δ and γ). It was found that the model exhibits a wealth of characteristic dynamical behavior, including stationary equilibria, bifurcations from stationary equilibria to periodic orbits, period doubling bifurcations, chaotic solutions on a strange attractor, tangent bifurcations from chaotic to periodic solutions, transient chaos, and hysteresis. It is not our purpose here to detail the behavior of this system. Rather, we wish to use it as an illustration of scale invariant nature in a strange attractor. For a range of the parameters δ and γ, this system exhibits chaotic time dependence with only a moderate phase-space volume contraction rate. Thus structure of the associated strange attractor is evident in the surface of section (Fig. 21). Furthermore, upon magnification, it is evi-

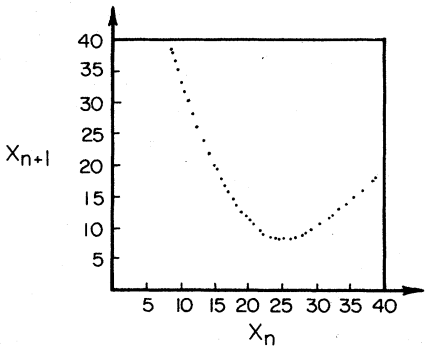

FIG. 20. Points x_{n+1} vs x_n lie approximately on a curve defining a one-dimensional map.

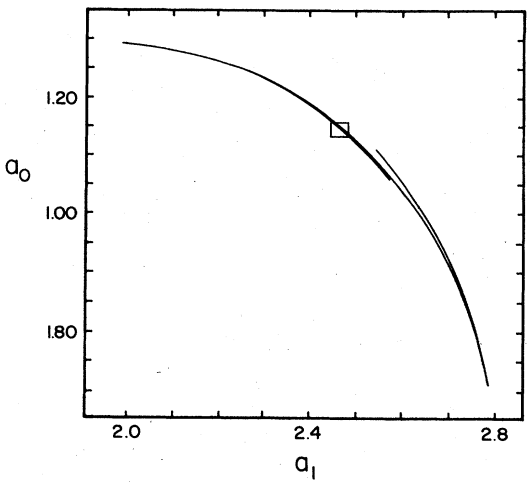

FIG. 21. Surface of section for a particular set of parameters for example (3).

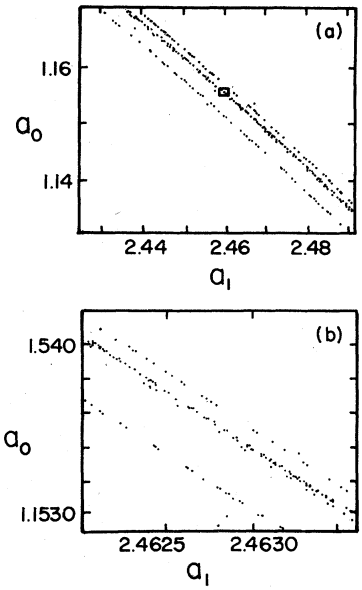

FIG. 22. (a) Magnification of the region in Fig. 21 shown in the rectangle, and (b) magnification of the rectangular region indicated in Fig. 22(a). Scale invariance is evident.

dent that the structure appears to be approximately scale invariant. This is illustrated in Fig. 22 which is to be considered analogous to Fig. 10 for the Henon map.

V. PARTIAL DIFFERENTIAL EQUATIONS, ORDINARY DIFFERENTIAL EQUATIONS, AND TURBULENCE

It is natural to ask whether the phenomena revealed by the examples of the preceding section carry over to more complicated systems. In particular, what happens if the restriction of phase-space volume contraction is lifted and if the dimension of the system is larger than three? Furthermore, the examples in Sec. IV were meant as approximate models for phenomena which are more exactly described only by partial differential equations. Partial differential equations may often be thought of as infinite systems of ordinary differential equations; e.g., it is frequently possible to expand the dependent variables of a partial differential equation in an infinite discrete set of Fourier spatial modes and to derive an infinite set of coupled nonlinear ordinary differential equations for the time dependence of the Fourier coefficients.

It seems clear that such more general systems might display the same characteristic phenomena as those discussed in Sec. IV, but could also reveal additional phenomena ruled out by the specific constraints adopted in Sec. IV. For example, we have found in Sec. IV cases where chaotic solutions occur for a strange attractor of dimension between two and three. For higher dimensional systems, strange attractors are possible with higher dimensionality—e.g., one might have a strange attractor of dimension between five and six if a system of n differential equations with $n \geq 6$ were investigated. (Such higher dimensional strange attractors might be quite difficult to diagnose in actual situations.) At any rate, it seems reasonable to suppose that, as a parameter which characterizes the strength of destabilizing forces in a system described by partial differential equations is cranked up (e.g., the Reynolds number), the general (although not uniform) tendency would be toward motion on attractors of increasing dimension. For example, a stable attracting stationary equilibrium point (zero-dimensional attractor) might bifurcate to a periodic orbit (one-dimensional attractor), which then proceeds via an infinite number of period doubling bifurcations to a strange attractor of dimension between two and three, which then becomes a strange attractor with dimension between three and four, etc. Another possible sequence might be a stationary point (zero dimensions) that bifurcates to a periodic orbit (one dimension), which bifurcates to a doubly periodic orbit (a two-dimensional attractor formed by the surface of a torus), which then bifurcates to a strange attractor (dimension> 2). The former route to a strange attractor [cf. Fig. 23(a)] has been demonstrated in Sec. IV.B.2. The route to a strange attractor via transition from a doubly periodic orbit (motion on a two-dimensional toroidal surface) is illustrated in Fig. 23(b) and was first discussed in a pioneering paper by Ruelle and Takens (1971) [cf. also Newhouse *et al.*, 1978). (Note that this route to a strange attractor [Fig. 23(b)] is specifically ruled out for the examples in Sec. IV, since, as previously mentioned, doubly periodic orbits are not possible in a system of three ordinary differential equations with phase-space contraction.)

Ruelle and Takens (1971) conjectured that small nonlinearities would destroy triply periodic motions. They therefore reasoned that, as the Reynolds number of a fluid flow is increased, the sequence in Fig. 23(b) ought to occur. In particular, they concluded that the last step, (doubly periodic motion) → (strange attractor), is quite likely, since doubly periodic motions cannot bifurcate to triply periodic motions if the latter are unstable. Although the reasoning leading to their conclusion that the onset of turbulence may be associated with a strange attractor is indirect, this paper and that of Lorenz are the first to point out the possible relevance of strange attractors in a physical context. Furthermore, their picture of turbulence onset is a fundamental departure from that advocated by Landau (1941) (cf. also Landau and Lifshitz, 1959). Landau argued that turbulence in fluid flow may be viewed as a hierarchy of instabilities. As the Reynolds number, R, is increased from zero, the basic state becomes unstable to a mode of frequency $\tilde{\omega}_1$ which saturates in a nonlinear periodic state for which dependent variables can be written in the form $\sum_l a_l \exp(-il\omega_1 t)$; as R is further increased, another instability appears at $\tilde{\omega}_2$ and the saturated state becomes doubly periodic, $\sum_{l,m} a_{lm} \times \exp(-il\omega_1 t - im\omega_2 t)$; further increase of R leads to the successive appearance of more and more discrete frequencies so that doubly periodic flow (ω_1, ω_2) transforms to triply periodic, then to quadruply periodic, etc. Thus, as R is increased, more and more frequencies are present, and the flow pattern becomes more and more complicated. Thus in this model the

(A)

STATIONARY POINT → BIFURCATION TO A PERIODIC ORBIT → PERIOD DOUBLING BIFURCATIONS → ACCUMULATION POINT OF AN INFINITE NUMBER OF PERIOD DOUBLING BIFURCATIONS → STRANGE ATTRACTOR

FIG. 23. Two possible routes to a strange attractor.

(B)

STATIONARY POINT → BIFURCATION TO A PERIODIC ORBIT → BIFURCATION TO A DOUBLY PERIODIC ORBIT → STRANGE ATTRACTOR

Fourier spectrum is always discrete and approximates a continuum only in the case where a large number of discrete frequencies are present. Furthermore, the flow is never truly chaotic, since the time correlation functions of multiply periodic functions do not tend to zero for large argument. On the other hand, the appearance of a strange attractor (as, for example, by the sequence of events in Fig. 23) can lead to turbulent motions in a direct way. Recent experiments on the onset of turbulence induced by various instabilities lend support to the idea that turbulence onset may be due to the appearance of a strange attractor (Swinney and Gollub, 1978; Ahlers and Behringer, 1978; Fenstermacher *et al.*, 1979; Walden and Donnelly, 1979; Lashinsky, 1980; Donnelly *et al.*, 1980; Moon and Holmes, 1980).

We now discuss some evidence that the sequence to a strange attractor via a route something like that depicted in Fig. 23(b) can occur. To begin we note the recent study by Curry (1978). In this paper, the author considers the same physical problem as that considered by Lorenz, but includes a greater number of Fourier spatial modes before truncating the series representation of the dependent variables. The result is a system of 14 coupled ordinary differential equations, rather than the three studied by Lorenz. The numerical results of Curry are somewhat different than those of Lorenz. In particular, he finds that chaotic time dependence is preceded by doubly periodic motion on a two-dimensional toroidal surface that is embedded in the full 14-dimensional phase space. The existence of the torus is found by using the surface of section technique: a surface of section $x_1 = \text{const}$ was chosen (where x_1 is one of the 14 variables), and another two of the 14 variables, which we denote by x_2 and x_3, were singled out. Every time the orbit crossed the surface of section the x_2, x_3 coordinates of the crossing point were plotted. Figure 24 shows a typical result for the case where a doubly periodic orbit exists. As can be seen from Fig. 24, the points lie on a closed curve. This is the result to be expected for doubly periodic behavior, since the intersection of a torus with a plane (the surface of section) is a closed curve. Related numerical studies have been performed by Yahata (1978) and Sherman and McLaughlin (1978).

Another relevant study is that of Curry and Yorke (1978), who consider a simple two-dimensional map that models the onset of chaos preceded by doubly periodic motion. The mapping that they study is one which may conveniently be represented as the result of two successive transformations, the first in polar coordinates

$$(\rho, \theta) \to [\varepsilon \ln(1+\rho), \theta + \theta_0] \tag{5.1a}$$

and the second in rectangular coordinates

$$(x, y) \to (x, y + x^2), \tag{5.1b}$$

where $\varepsilon \geq 0$ and $\theta_0 \geq 0$ are parameters to be chosen. Note that for $\varepsilon > 1$, the mapping $\rho \to \varepsilon \ln(1+\rho)$ has two fixed points, one of which is $\rho = 0$ and the other of which (denoted by ρ_ε) is the positive root of $\rho_\varepsilon = \varepsilon \ln(1+\rho_\varepsilon)$. For $1 \geq \varepsilon > 0$, the only fixed point is $\rho = 0$. Consider first the iteration of the polar map, $(\rho, \theta) \to [\varepsilon \ln(1+\rho), \theta + \theta_0]$, alone. For $\varepsilon > 1$, all points tend asymptotically to the circle $\rho = \rho_\varepsilon > 0$. Furthermore, if the rotation angle θ_0 is not 2π times a rational number, then the orbit fills up the entire circle $\rho = \rho_\varepsilon$. As ε approaches one from above, $\rho_\varepsilon \to 0$, so that is may be considered that this map undergoes a bifurcation from a stable fixed point to an attracting orbit on the circle $\rho = \rho_\varepsilon$.

Thus the map $(\rho, \theta) \to [\varepsilon \ln(1+\rho), \theta + \theta_0]$ can be viewed as modeling a surface of section for some differential equation that undergoes a bifurcation of a stable periodic orbit to a doubly periodic orbit on a torus (where $\rho = \rho_\varepsilon$ represents the intersection of this torus with the surface of section and $\rho = 0$ represents the intersection of the periodic orbit with the surface of section).

For ε only slightly larger than one, $\rho_\varepsilon \ll 1$, and the map $(x, y) \to (x, y + x^2)$ is almost the identity map, since

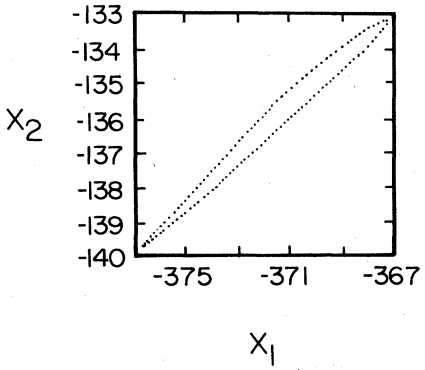

FIG. 24. Orbit intersections with the surface of section, obtained by Curry (1978).

the quadratic term, x^2, is comparatively small. Thus if one considers the map resulting from the successive application of the two above-mentioned transformations, then for $\varepsilon > 1$ the map $(x, y) \to (x, y + x^2)$ introduces a nonlinearity that becomes stronger as ε is increased. Curry and Yorke have described a sequence of numerical studies of the attracting set for the composite map, Eqs. (5.1), with $\theta_0 = 2$. At $\varepsilon = 1.01$ a nearly circular loop encircles the origin. As ε increases, the loop distorts and increases in size until $\varepsilon = 1.28$. For $1.39 \gtrsim \varepsilon > 1.28$ an attracting period three orbit is found. Immediately after $\varepsilon \cong 1.3953$, an apparently connected loop returns. This apparent loop, however, actually has a complicated structure and is, in fact, a strange attractor.

As ε increases somewhat, the strange aspect of the attractor becomes more apparent, as evidenced by Fig. 25 for $\varepsilon = 1.45$. The bump containing the point P_1 in Fig. 25 is mapped to P_2, to P_3, to P_4, ... to P_{11}. The cusplike structure at P_4 shows signs of being flattened against the rest of the set. Each successive cusp is more flattened and more elongated. Soon the cusps are so flattened that they are no longer discernable. This sequence, P_i, is, however, infinite. Note, too, that the successive elongation of the cusps represents a stretching apart of two nearby points. As discussed in Sec. III, such stretching should be expected to lead to chaotic behavior, and this is in fact the case here. Similar behavior has also been observed in a map studied by Coullet *et al.* (1980).

The character of the strange attractor for the example of Curry and Yorke appears to be that of a very complicated curve folded over on itself an infinite number of times and with an infinite length. In this connection, it may be of some interest to give a simple example of an infinite length curve with Hausdorf dimension between one and two (Mandelbrot, 1977). Consider the sequence of operations shown in Fig. 26. We start with an equilateral triangle, divide each of the sides in thirds, and erect smaller equilateral triangles on the middle thirds on each side. The process is repeated twice in the figure. On each application of the process the length of the bounding curve increases by $\frac{4}{3}$. In the limit that the process is repeated an infinite number of times, the length of the bounding curve approaches infinity, although the curve remains in a bounded region of the plane. Furthermore, it may be verified that the Hausdorf dimension of this curve is $\ln 4/\ln 3 \cong 1.26$.

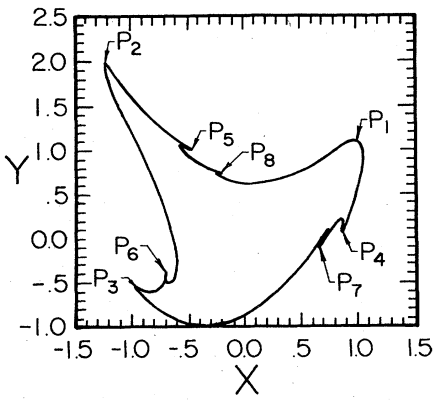

FIG. 25. The attractor for the map of Curry and Yorke with $\theta_0 = 2$ and $\varepsilon = 1.45$.

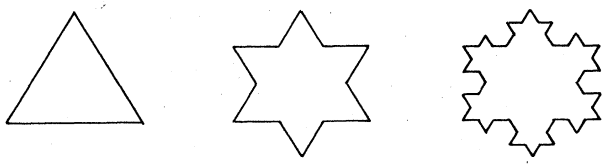

FIG. 26. Illustration of the construction of a curve of dimension $\ln 4/\ln 3$.

VI. CONCLUSIONS

This subject matter is certain to receive much future attention from researchers in the physical sciences and in mathematics. It seems clear that there is a great need for further work in order that the subject develop to the point that theory can provide answers to many of the most practical questions. For example, given a system of equations, can one predict the occurrence of a strange attractor? To what extent can properties of the strange attractor such as its dimension, associated distribution function, power spectra, and correlation functions be predicted? What is the distribution function on a strange attractor and what is the most efficient way to find it and characterize it? Further work will also certainly be done identifying physical systems which exhibit chaotic motions associated with strange attractors. The list of such systems (partially enumerated in the Introduction) is already impressive, and, as it grows, it is to be expected that interest on the part of physical scientists will also grow.

ACKNOWLEDGMENTS

The author wishes to thank Professor J. A. Yorke for many informative discussions. This work was supported by the U. S. Department of Energy.

REFERENCES

Adam, J. C., M. N. Bussac, and G. Laval, 1980, in *Intrinsic Stochasticity in Plasmas*, edited by G. Laval and D. Gresillon (Les Editions de Physique Courtaboeuf, Orsay, France), p. 415.

Afraymovich, V. S., V. V. Bykov, and L. P. Shilnikov, 1977, Dokl. Adak. Nauk, SSSR **234**, 336.

Ahlers, G., and R. P. Behringer, 1978, Phys. Rev. Lett. **40**, 712.

Bridges, R., and G. Rowlands, 1977, Phys. Lett. A **63**, 189.

Bunimovich, L. A., and Ya. G. Sinai, 1977, in *Proceedings of the Spring School on Nonlinear Waves, Gorki, U.S.S.R.*

Chang, S.-J., and J. Wright, 1981, Phys. Rev. **23**, 1419.

Chirikov, B. V., 1979, Phys. Rep. **52**, 463.

Coullet, P., and J.-P. Eckmann, 1980, *Iterated Maps on the Interval as Dynamical Systems* (Birkhauser, Boston).

Coullet, P., and C. Tresser, 1980, J. Phys. (Paris), Lett. **41**, L255.

Coullet, P., C. Tesser, and A. Arneodo, 1980, Phys. Lett. A **77**, 327.

Crutchfield, J., D. Farmer, N. Packard, R. Shaw, G. Jones, and R. J. Donnelly, 1980, Phys. Lett. A **76**, 1.

Crutchfield, J., M. Nauenberg, and J. Rudnick, 1981, Phys.

Rev. Lett. **46**, 933.
Curry, J. H., 1979, Commun. Math. Phys. **68**, 129.
Curry, J. H., and J. A. Yorke, 1978, in *The Structure of Attractors in Dynamical Systems*, edited by N. G. Markley, J. C. Martin, and W. Perrizo, Lecture Notes in Mathematics (Springer, Berlin), Vol. 668, p. 48.
Donnelly, R. J., K. Park, R. Shaw, and R. W. Walden, 1980, Phys. Rev. Lett. **44**, 987.
Feigenbaum, M. J., 1978, J. Stat. Phys. **19**, 25.
Feigenbaum, M. J., 1979, Phys. Lett. A **74**, 375.
Feit, S. D., 1978, Commun. Math. Phys. **61**, 249.
Fenstermacher, P. R., H. L. Swinney, and J. P. Gollub, 1979, J. Fluid Mech. **94**, 103.
Frederickson, P., J. L. Kaplan, and J. A. Yorke, 1980, preprint.
Greene, J. M., R. S. MacKay, F. Vivaldi, and M. J. Feigenbaum, 1981, preprint.
Greene, J. M., 1979, J. Math. Phys. **20**, 1183.
Guckenheimer, J., 1979, Commun. Math. Phys. **70**, 133.
Guckenheimer, J., G. Oster, and Ipaktchi, 1977, J. Math. Biol. **4**, 101.
Haken, H., 1975, Phys. Lett. A **53**, 77.
Helleman, R. H. G., 1980, in *Fundamental Problems in Statistical Mechanics 5*, edited by E. G. D. Cohen (North-Holland, Amsterdam), p. 165.
Henon, M., 1976, Commun. Math. Phys. **50**, 69.
Hirsch, M. W., and S. Smale, 1974, *Differential Equations, Dynamical Systems and Linear Algebra* (Academic, New York).
Holmes, P. J., 1977, Appl. Math. Modeling **1**, 362.
Holmes, P. J., 1980, preprint.
Huberman, B. A., and J. P. Cruchfield, 1979, Phys. Rev. Lett. **43**, 1743.
Huberman, B. A., and J. Rudnick, 1980, Phys. Rev. Lett. **45**, 154.
Huberman, B. A., and A. B. Zisook, 1981, Phys. Rev. Lett. **46**, 626.
Kaplan, J. L., and J. A. Yorke, 1979a, in *Functional differential Equations and Approximation of Fixed Points*, edited by H.-O. Peitzen and H.-O. Walther, Lecture Notes in Mathematics (Springer, Berlin), Vol. 730, p. 228.
Kaplan, J. L., and J. A. Yorke, 1979b, Commun. Math. Phys. **67**, 93.
Landau, L. D., 1941, C. R. (Dokl.) Acad. Sci. URSS **44**, 311.
Landau, L. D., and E. M. Lifshitz, 1959, *Fluid Mechanics* (Pergamon, London), Chap. 3.
Lanford, O. E., III, 1976, in *Statistical Mechanics and Dynamical Systems* (Mathematics Department, Duke University, Durham, North Carolina), Chap. 4.
Lashinsky, J., in *Intrinsic Stochasticity in Plasmas*, 1980, edited by G. Laval and D. Gresillon (Les Editions de Physique Courtaboeuf, Orsay, France), p. 425.
Li, T.-Y., and J. A. Yorke, Am. Math. Mon. **82**, 985 (1975).
Lorentz, E. N., 1979, presentation at the International Conference on Nonlinear Dynamics, New York Academy of Sciences (unpublished).
Lorenz, E. N., 1963, J. Atmos. Sci. **20**, 130.
Lozi, R., 1978, J. Phys. (Paris) Suppl. 8, tome 35, p. C5–9.
Mandelbrot, B. B., 1977, *Fractals* (Freeman, San Francisco).
Maschke, E. K., and B. Saramito, 1980, in *Intrinsic Stochasticity in Plasmas*, edited by G. Laval and D. Gresillon (Les Editions de Physique Courtaboeuf, Orsay, France), p. 383.
Masui, K., and P. K. C. Wang, 1980 (unpublished).
May, R. M., 1976, Nature **261**, 459.
McLaughlin, J., 1979, Phys. Rev. A **20**, 2114.
McLaughlin, J. B., and P. C. Martin, 1975, Phys. Rev. A **12**, 186.
Moon, F. C., and P. J. Holmes, 1979, J. Sound Vib. **65**, 275.
Newhouse, S., D. Ruelle, and F. Takens, 1978, Commun. Math. Phys. **64**, 35.
Rabinovitch, M. I., 1978, Sov. Phys.—Usp. **21**, 443.
Rechester, A. B., and T. H. Stix, 1976, Phys. Rev. Lett. **35**, 597.
Robbins, K. A., 1977, Math. Proc. Cambridge Philos. Soc. **82**, 209.
Rosenbluth, M. N., R. Z. Sagdeev, J. B. Taylor, and G. M. Zaslavskii, 1966, Nucl. Fusion **6**, 297.
Ruelle, D., 1977, in *Mathematical Problems in Theoretical Physics*, edited by G. Dell'Antonio, S. Doplicher, and G. Jona-Lasinio, Lecture Notes in Physics (Springer, Berlin), Vol. 80, p. 341.
Ruelle, D., and F. Takens, 1971, Commun. Math. Phys. **20**, 167.
Russell, D. A., J. D. Hanson, and E. Ott, 1980, Phys. Rev. Lett. **45**, 1175.
Russell, D. A., and E. Ott, 1980, preprint.
Saltzman, B., 1962, J. Atmos. Sci. **19**, 329.
Shaw, R., 1981, Z. Naturforsch. A **36**, 80.
Sherman, J., and J. B. McLaughlin, 1978, Commun. Math. Phys. **58**, 9.
Shimzu, T., and N. Morioda, 1978, Phys. Lett. A **69**, 148.
Shraiman, B., C. E. Wayne, and P. C. Martin, 1981, Phys. Rev. Lett. **46**, 935.
Simó, 1979, J. Stat. Phys. **21**, 465.
Sinai, Ya. G., 1977, in *Proceedings of the Spring School on Nonlinear Waves, Gorki, U.S.S.R.*
Stix, T. H., 1973, Phys. Rev. Lett. **30**, 833.
Swinney, H. L., and J. P. Gollub, 1978, Phys. Today **31** (8), 41.
Tomita, K., and T. Kai, 1979, J. Stat. Phys. **21**, 65.
Treve, Y., 1978, in *Topics in Nonlinear Dynamics*, edited by S. Jorna, AIP Conference Proceedings (American Institute of Physics, New York), no. 46, p. 147.
Treve, Y., and O. P. Manley, 1980, in *Intrinsic Stochasticity in Plasmas*, edited by G. Laval and D. Gresillon (Les Editions de Physique Courtaboeuf, Orsay, France), p. 393.
Vyshkind, S. Ya., 1978, Radiofizika **21**, 850 [Sov. Radiophys. **21**, 600].
Vyshkind, S. Ya., and M. I. Rabinovich, 1976, Zh. Eksp. Teor. Fiz. **71**, 557 [Sov. Phys.—JETP **44**, 292 (1976)].
Walden, R. W., and R. J. Donnelly, 1979, Phys. Rev. Lett. **42**, 301.
Wang, P. K. C., 1980, J. Math. Phys. **21**, 398.
Wersinger, J. M., J. M. Finn, and E. Ott, 1980a, in *Intrinsic Stochasticity in Plasmas*, edited by G. Laval and D. Gresillon (Les Editions de Physique Courtaboeuf, Orsay, France), p. 403.
Wersinger, J. M., J. M. Finn, and E. Ott, 1980b, Phys. Rev. Lett. **44**, 453.
Wersinger, J. M., J. M. Finn, and E. Ott, 1980c, Phys. Fluids **23**, 1142.
Wolf, A., and J. Swift, 1981, preprint.
Yahata, H., 1978, Prog. Theor. Phys. Suppl. **64**, 165.
Yorke, J. A., and E. D. Yorke, 1979, J. Stat. Phys. **21**, 263.
Yorke, J. A., and E. D. Yorke, 1981, in *Hydrodynamic Instabilities and the Transition to Turbulence*, edited by H. L. Swinney and J. P. Gollub (Springer, Berlin), p. 77.
Zaslavskii, G. M., 1978, Phys. Lett. A **69**, 145.
Zaslavskii, G. M., and Kh.-R. Ya Rachko, 1979, Zh. Eksp. Teor. Fiz. **76**, 2052 [Sov. Phys.—JETP **49**, 1039 (1979)].